Translational Oncology
www.transonc.com

Volume 9 Number 3 June 2016 pp. 211–218 211

Intracranial Tumor Cell Migration and the Development of Multiple Brain Metastases in Malignant Melanoma[1,2]

Trude G. Simonsen, Jon-Vidar Gaustad and Einar K. Rofstad

Group of Radiation Biology and Tumor Physiology, Department of Radiation Biology, Institute for Cancer Research, Oslo University Hospital, Oslo, Norway

Abstract

INTRODUCTION: A majority of patients with melanoma brain metastases develop multiple lesions, and these patients show particularly poor prognosis. To develop improved treatment strategies, detailed insights into the biology of melanoma brain metastases, and particularly the development of multiple lesions, are needed. The purpose of this preclinical investigation was to study melanoma cell migration within the brain after cell injection into a well-defined intracerebral site. *METHODS:* A-07, D-12, R-18, and U-25 human melanoma cells transfected with green fluorescent protein were injected stereotactically into the right cerebral hemisphere of nude mice. Moribund mice were killed and autopsied, and the brain was evaluated by fluorescence imaging or histological examination. *RESULTS:* Intracerebral inoculation of melanoma cells produced multiple lesions involving all regions of the brain, suggesting that the cells were able to migrate over substantial distances within the brain. Multiple modes of transport were identified, and all transport modes were observed in all four melanoma lines. Thus, the melanoma cells were passively transported via the flow of cerebrospinal fluid in the meninges and ventricles, they migrated actively along leptomeningeal and brain parenchymal blood vessels, and they migrated actively along the surfaces separating different brain compartments. *CONCLUSION:* Migration of melanoma cells after initial arrest, extravasation, and growth at a single location within the brain may contribute significantly to the development of multiple melanoma brain metastases.

Translational Oncology (2016) 9, 211–218

Introduction

Brain metastasis is a frequent and fatal complication of malignant melanoma, and 20% to 55% of patients with metastatic melanoma die as a result of their brain metastases [1–3]. Melanoma brain metastases are generally resistant to both radiation and chemotherapy, and furthermore, they are characteristically multifocal and are therefore difficult to treat with surgical resection [4]. Clinical studies have reported that approximately 60% of melanoma patients diagnosed with brain metastases develop multiple brain lesions, and these patients show particularly poor prognosis [5–7]. To develop improved treatment strategies for these patients, detailed insights into the biology of melanoma brain metastases, and particularly the development of multiple brain lesions, are highly needed.

Multiple brain metastases may arise from multiple tumor cells entering the brain from the arterial circulation at different times and at different locations within the brain. Alternatively, they may arise as a result of tumor cell migration within the brain after initial arrest, extravasation, and growth at a single location. Preclinical studies have demonstrated that melanoma cells can be highly motile within the brain and can migrate actively along the external surface of brain microvessels [8–10]. Carbonell et al. have suggested that this type of migration relies on β1 integrin-mediated tumor cell adhesion to the

Address all correspondence to: Einar K. Rofstad, Department of Radiation Biology, Institute for Cancer Research, Norwegian Radium Hospital, Box 4953 Nydalen, N-0424, Oslo, Norway.
E-mail: einar.k.rofstad@rr-research.no

[1] Conflicts of interest: none.

[2] Financial support was received from the Norwegian Cancer Society and the South-Eastern Norway Regional Health Authority. The funding sources had no role in study design; in the collection, analysis, and interpretation of data; in the writing of the report; and in the decision to submit the article for publication.
Received 23 January 2016; Revised 7 April 2016; Accepted 10 April 2016

1936-5233/16
http://dx.doi.org/10.1016/j.tranon.2016.04.003

vascular basement membrane [9]. Furthermore, invasive growth of melanoma cells along brain microvessels has been observed in studies of patient biopsies and autopsy specimens [11,12]. These data suggest that migration of melanoma cells away from an original metastatic site within the brain may contribute to the development of multiple brain lesions in melanoma patients. However, most studies have detected melanoma cell migration across relatively short distances within the brain, and preclinical data are mainly derived from studies where tumor cells were injected into the arterial circulation, thus making it difficult to determine the origin of individual brain lesions.

In the study reported here, we injected human melanoma cells transfected with green fluorescent protein (GFP) into a well-defined site in the right cerebral hemisphere of nude mice by using a stereotactic device. Moribund mice were killed and autopsied, and melanoma cells within the brain were detected by GFP fluorescence imaging or by GFP immunohistochemistry. Multiple melanoma lesions involving brain regions far from the injection site were detected, and we identified multiple modes of melanoma cell transport within the brain.

Materials and Methods

Mice

Adult (8-10 weeks of age) female BALB/c *nu/nu* mice were used as host animals. The mice were bred at our institute and maintained under specific pathogen-free conditions at a temperature of 22°C to 24°C and a humidity of 30% to 50%. The animal experiments were approved by the Institutional Committee on Research Animal Care and were performed according to the Interdisciplinary Principles and Guidelines for the Use of Animals in Research, Marketing, and Education (New York Academy of Sciences, New York, NY).

Cell Lines

Intracerebral tumors were initiated from the A-07, D-12, R-18, and U-25 human melanoma cell lines [13]. When these lines were established, large stocks of cells were frozen and stored in liquid nitrogen. Cells derived directly from the frozen stocks were constitutively transfected with GFP by lipofection using the pEGFP-N1 plasmid (Clontech Laboraories, Mountain View, CA) as described elsewhere [14]. Frozen stocks of cell clones showing high and stable GFP expression were established, and the GFP transfected cell cultures used in the experiments described here were initiated from these frozen stocks. Monolayer cultures were incubated at 37°C in a humidified atmosphere of 5% CO_2 in air and subcultured twice a week in RPMI 1640 (25 mM HEPES and L-glutamine) medium. The medium was supplemented with 13% bovine calf serum; 250 µg/ml of penicillin; 50 µg/ml of streptomycin; and 700 µg/ml (A-07), 900 µg/ml (D-12), 2200 µg/ml (R-18), or 1200 µg/ml (U-25) of genetecin. However, genetecin selection may not have been necessary because we have revealed that the cells show high GFP expression even when grown for 3 months in medium without genetecin. By initiating new cell cultures from the frozen stocks at regular short intervals, we ensured that the experiments were not influenced by changes in the characteristics of the cell lines that may be induced during long-term culture *in vitro*.

Anesthesia

Intracerebral injection of tumor cells was carried out with anesthetized mice. Fentanyl citrate (Janssen Pharmaceutica, Beerse, Belgium), fluanisone (Janssen Pharmaceutica), and midazolam (Hoffmann-La Roche, Basel, Switzerland) were administered intraperitoneally in doses of 0.63 mg/kg, 20 mg/kg, and 10 mg/kg, respectively. The body core temperature of the mice was maintained at 37°C to 38°C by using a heating pad.

Intracerebral Tumor Cell Inoculation

The mice were fixed in a stereotactic apparatus (Model 900; Kopf Instruments, Tujunga, CA) for inoculation of tumor cells into the right cerebral hemisphere. The injection point was 2 mm anterior to the coronal and 1 mm lateral to the sagittal suture lines (Figure 1). The immediate mouse mortality and the development of neurological signs shortly after cell inoculation have been shown to be low by using this injection point [15]. A 100-µl Hamilton syringe with a 26-gauge needle was used to inject 3.0×10^3 tumor cells suspended in 6 µl of Ca^{2+}-free and Mg^{2+}-free Hanks' balanced salt solution at a depth of 3.0 mm below the skull. To minimize tumor cell reflux, the cells were injected slowly, and the needle was left in place for 2 minutes before it was retracted slowly, as suggested by Fidler [15]. Twenty mice of each

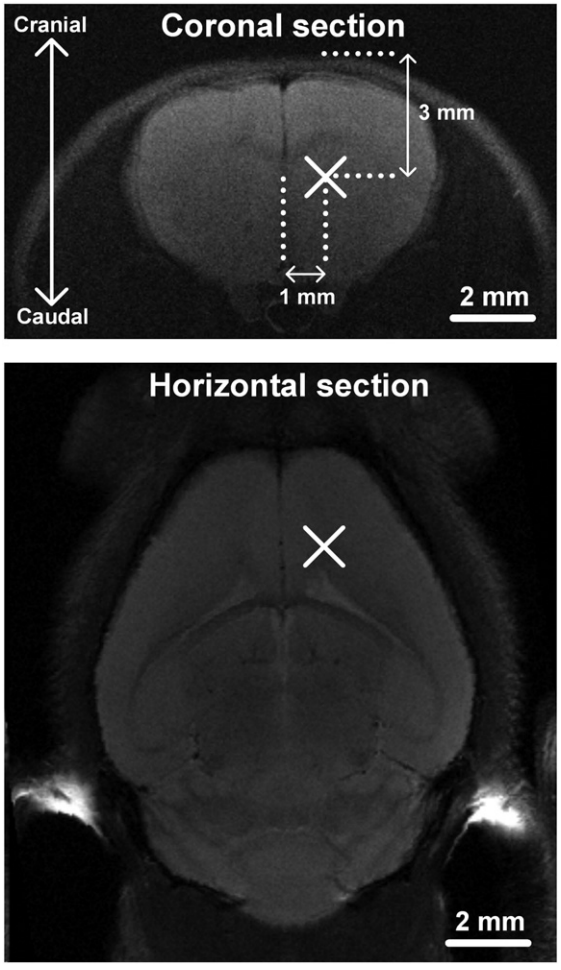

Figure 1. T_2-weighted magnetic resonance (MR) images of the mouse brain illustrating the cell inoculation site (cross) located 1 mm lateral to the sagittal suture lines and 3 mm caudal to the skull. The images show a coronal (top) and a horizontal section (bottom), and were recorded by using a 7.05-T Bruker small-animal MR scanner and a fast spin echo pulse sequence with a repetition time of 2200 milliseconds and an echo time of 36 milliseconds.

melanoma line were included in the study. The mice were examined daily for up to 70 days after tumor cell injection. Moribund mice were killed and autopsied, and the brain was removed for subsequent fluorescence imaging or histological analysis. The mice were defined to be moribund when they showed a weight loss of 20% or when the skull sutures were disconnected because of intracranial tumor growth.

Fluorescence Imaging

Imaging was performed with an inverted fluorescence microscope equipped with a filter for green light (IX-71; Olympus, Munich, Germany), a black-and-white CCD camera (C4742-95; Hamamatsu Photonics, Hamamatsu, Japan), and appropriate image acquisition software (Wasabi, Hamamatsu Photonics). The fresh brain was imaged immediately after autopsy. The cranial and caudal surfaces of the brain as well as three coronal brain sections with a thickness of ~2 mm were imaged at low (×2) and high (×4-×10) magnifications (Figures 1 and 2, *A*).

Histological Analysis

The brain was fixed in phosphate-buffered 4% paraformaldehyde. Histological coronal brain sections were stained with hematoxylin and eosin (HE) by using a standard procedure or immunostained by using

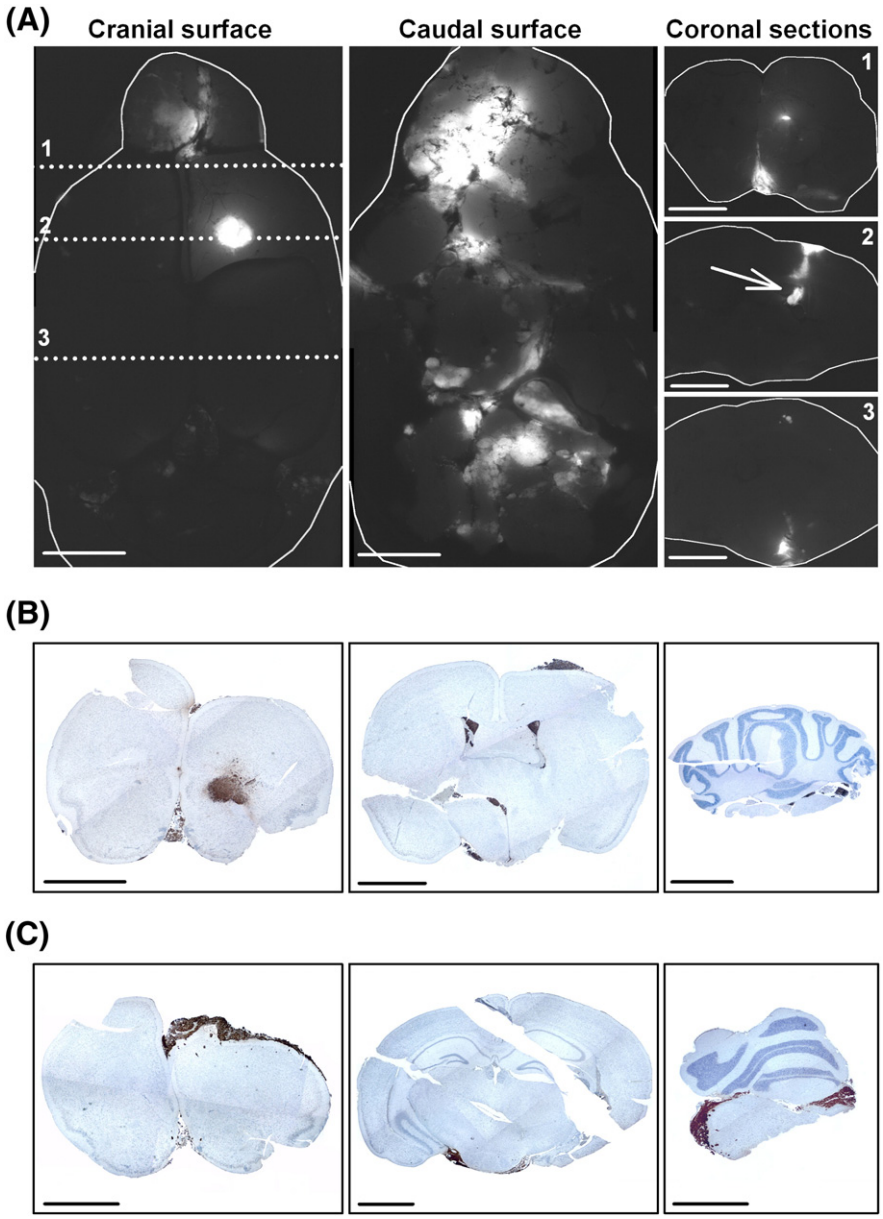

Figure 2. Multiple brain lesions after intracerebral injection of GFP-expressing melanoma cells visualized by fluorescence imaging and GFP immunohistochemistry. (A) GFP fluorescence images of the cranial surface, the caudal surface, and three coronal sections of the brain obtained 4 weeks after injection of R-18 cells. Dotted lines indicate the positions of the coronal brain sections. Arrow indicates the injection site. (B) GFP-stained histological brain sections showing R-18 cells at the injection site (left panel), in the lateral ventricles (middle panel), and between the cerebellum and the brain stem (right panel). (C) GFP-stained histological brain sections showing D-12 cells in the leptomeningeal linings of the right cerebral hemisphere (left panel), the midbrain (middle panel), and the brain stem and cerebellum (right panel). Scale bars, 2 mm.

a peroxidase-based indirect staining method [16]. An anti-GFP rabbit polyclonal antibody or an anti-CD31 rabbit polyclonal antibody (Abcam, Cambridge, United Kingdom) was used as primary antibody to detect tumor cells or endothelial cells respectively. Diaminobenzidine was used as chromogen, and hematoxylin was used for counterstaining.

Statistical Analysis

Comparisons of data were carried out by one-way analysis of variance followed by Bonferroni's test. The Kolmogorov-Smirnov method and the Levene's method were used to verify that the data complied with the conditions of normality and equal variance. Probability values of $P < .05$, determined from two-sided tests, were considered significant. The statistical analysis was carried out with SigmaStat statistical software.

Results and Discussion

Multiple Brain Lesions following Intracerebral Inoculation of Melanoma Cells

To study melanoma cell migration within the brain, GFP-expressing A-07, D-12, R-18, and U-25 cells were injected stereotactically into the right cerebral hemisphere of nude mice. Clinical symptoms of intracranial tumor growth were evident within 2 to 5 weeks, and the intracranial growth pattern was evaluated by fluorescence imaging or by GFP immunohistochemistry. Figure 2, *A* shows examples of fluorescence images of a brain obtained 4 weeks after injection. GFP-expressing melanoma cells were present at the injection site, on the cranial and caudal brain surfaces, and in coronal brain sections anterior and posterior to the injection site. Similar patterns of multiple melanoma lesions were observed in GFP-stained histological sections, as illustrated in Figure 2, *B* and *C*. Histological sections revealed melanoma lesions located in the injection site (Figure 2, *B*, *left panel*), in the ventricles (Figure 2, B, *middle panel*), in areas between different brain compartments (Figure 2, *B*, *right panel*), and in the leptomeningeal lining of various brain regions, including the cerebrum, midbrain, brain stem, and cerebellum (Figure 2c).

Because the cells were injected into one well-defined intracerebral site, the observed pattern of multiple melanoma lesions involving brain compartments far from the injection site shows that the melanoma cells were able to migrate across substantial distances within the brain. Moreover, melanoma lesions were frequently located in the ventricles or in the leptomeninges, thus suggesting that the melanoma cells used these brain compartments as transport routes. The A-07, D-12, R-18, and U-25 cell lines were all established from subcutaneous metastases [13], and previous studies have demonstrated that human melanoma cell lines established from subcutaneous or lymph node metastases produce metastases mainly in the meninges and ventricles following intra-arterial injection [17,18]. Furthermore, meningeal involvement has been observed in 7% to 23% of patients with melanoma brain metastases and was identified as an important negative prognostic factor in multiple clinical studies [6,7,19,20].

Passive Transport of Melanoma Cells via the Flow of Cerebrospinal Fluid in the Meninges and Ventricles

In mice showing intraventricular tumor growth, melanoma lesions were observed within multiple intraventricular spaces. This is illustrated in Figure 3, *A* showing intraventricular melanoma lesions within the two lateral ventricles, the third ventricle, and the fourth ventricle. Furthermore, leptomeningeal tumor deposits were frequently observed within the characteristic folds on the surface of the cerebellum (Figure 3, *B*). The interconnected ventricular spaces and the subarachnoid spaces within the meninges are filled with cerebrospinal fluid (CSF), and it is well recognized that tumor cells can spread through these spaces by passive transport via CSF flow [21]. Thus, in patients with leptomeningeal involvement, tumor deposits are frequently observed in areas characterized by slow CSF flow, including the cerebral basal cisterns, the cauda equina, and the folded surface of the cerebellum [22]. The melanoma lesions observed within the ventricular system and within the folds on the surface of the cerebellum in the present study were thus in accordance with previous studies and suggest that passive transport of melanoma cells via CSF flow in the meninges and ventricles is an important transport route for melanoma cells within the brain.

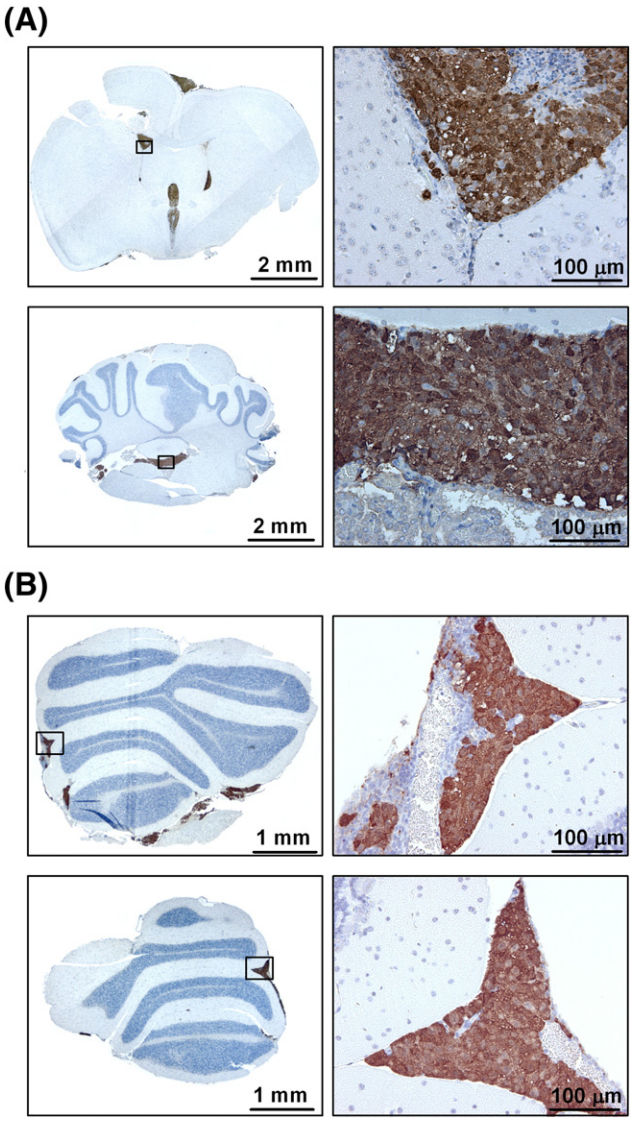

Figure 3. GFP-stained histological brain sections showing melanoma lesions resulting from passive transport of tumor cells through the cerebrospinal fluid. (A) R-18 cells within the two lateral ventricles and the third ventricle (upper panels), and within the fourth ventricle (lower panels). (B) R-18 cells within the folds on the surface of the cerebellum. High-magnification images show areas indicated by squares in the low-magnification images.

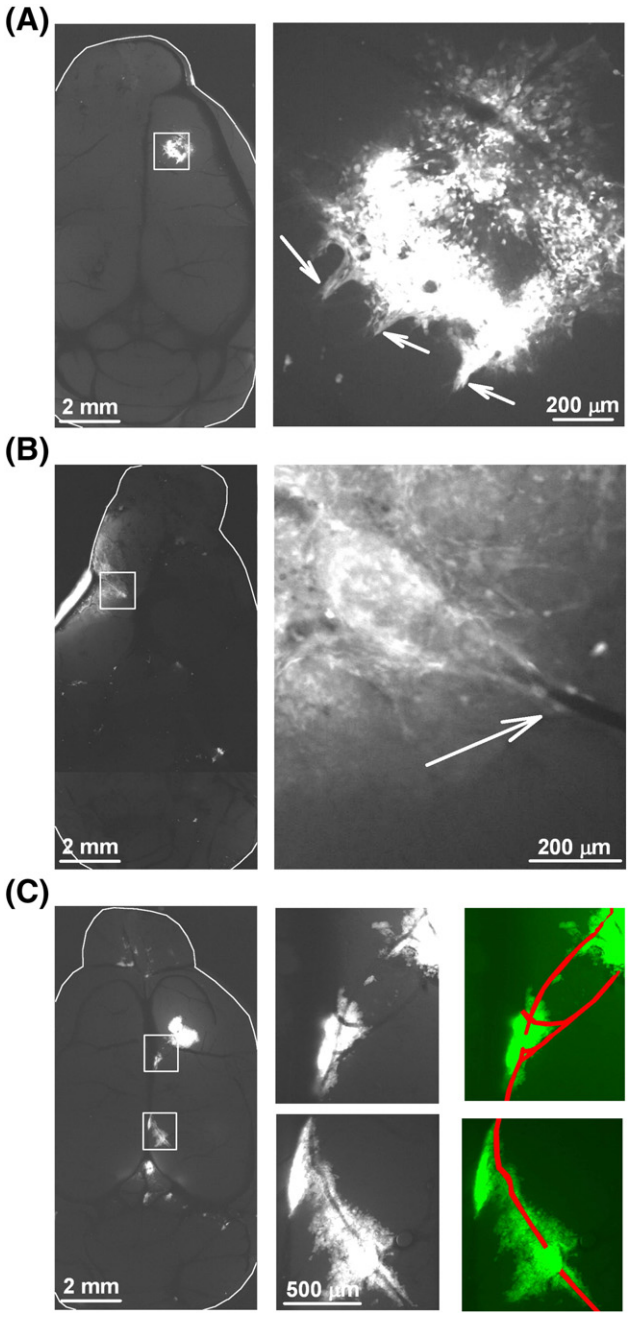

Figure 4. Fluorescence images showing migration of GFP-expressing melanoma cells along leptomeningeal blood vessels on the brain surface. (A) D-12 cells migrating along multiple blood vessels (arrows) away from a larger tumor lesion in the leptomeninges. (B) D-12 cells migrating along a blood vessel (arrow) on the caudal brain surface. (C) R-18 cells migrating along a blood vessel on the cranial brain surface. Blood vessels are visible in the fluorescence images because of the negative contrast of the red blood cells. High-magnification images show areas indicated by squares in the low-magnification images. Right panels of (C) show a schematic illustration of the high-resolution fluorescence images and show blood vessels in red and GFP-expressing tumor cells in green.

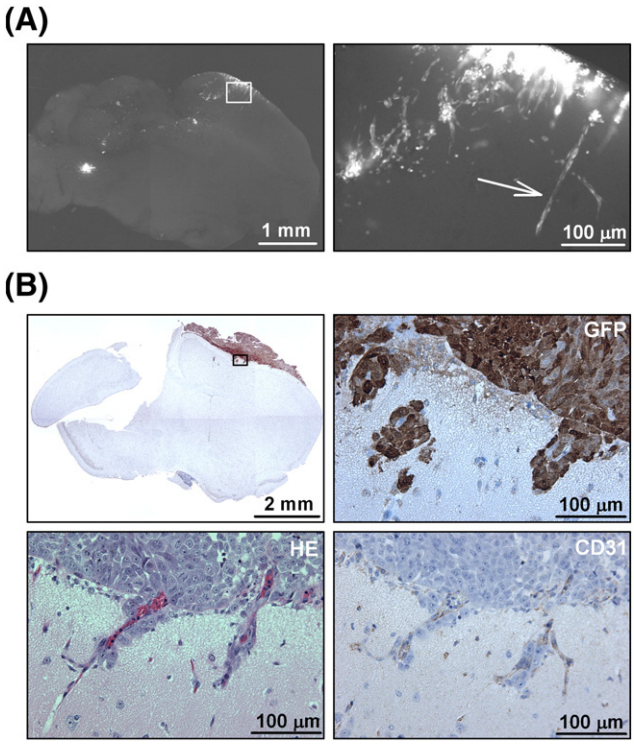

Figure 5. Melanoma cell invasion of the brain parenchyma along blood vessels entering the brain from the leptomeninges. (A) Fluorescence images showing GFP-expressing U-25 cells in a coronal brain section. Arrow indicates blood vessel. High-magnification image shows area indicated by a square in the low-magnification image. (B) Histological brain sections showing GFP-expressing D-12 cells. High-resolution images show a GFP-stained, an HE-stained, and a CD31-stained histological section of the area indicated by a square in the low-resolution GFP-stained section.

Active Migration of Melanoma Cells along Leptomeningeal and Parenchymal Blood Vessels

High-resolution fluorescence images revealed that melanoma cells migrated actively along leptomeningeal blood vessels on the brain surface. Three different examples are presented in Figure 4. Figure 4, *A* shows melanoma cell migration along multiple leptomeningeal blood vessels leading away from a larger lesion in the leptomeninges; Figure 4, *B* shows melanoma cell migration along a blood vessel on the caudal brain surface; and Figure 4, *C* shows melanoma cell migration along a blood vessel on the cranial brain surface. Furthermore, melanoma cells also migrated along blood vessels within the brain parenchyma. This is illustrated in Figure 5 showing fluorescence images of a coronal brain section (Figure 5, *A*) and GFP-stained, HE-stained, and CD31-stained histological brain sections (Figure 5, *B*) showing melanoma cells migrating along blood vessels entering the brain parenchyma from the leptomeninges. Our data are consistent with previous studies demonstrating melanoma cell migration along blood vessels within the brain [8,9,11], and moreover, they show that melanoma cells are able to migrate actively along blood vessels across substantial distances.

Active Migration of Melanoma Cells along the Surfaces Separating Different Brain Compartments

GFP-stained histological sections revealed multiple small colonies of melanoma cells located in the surfaces separating different brain compartments. Figure 6, *A* shows an example of two small melanoma cell colonies along the surfaces separating the right and left cerebral hemispheres. Interestingly, they are located between two larger lesions

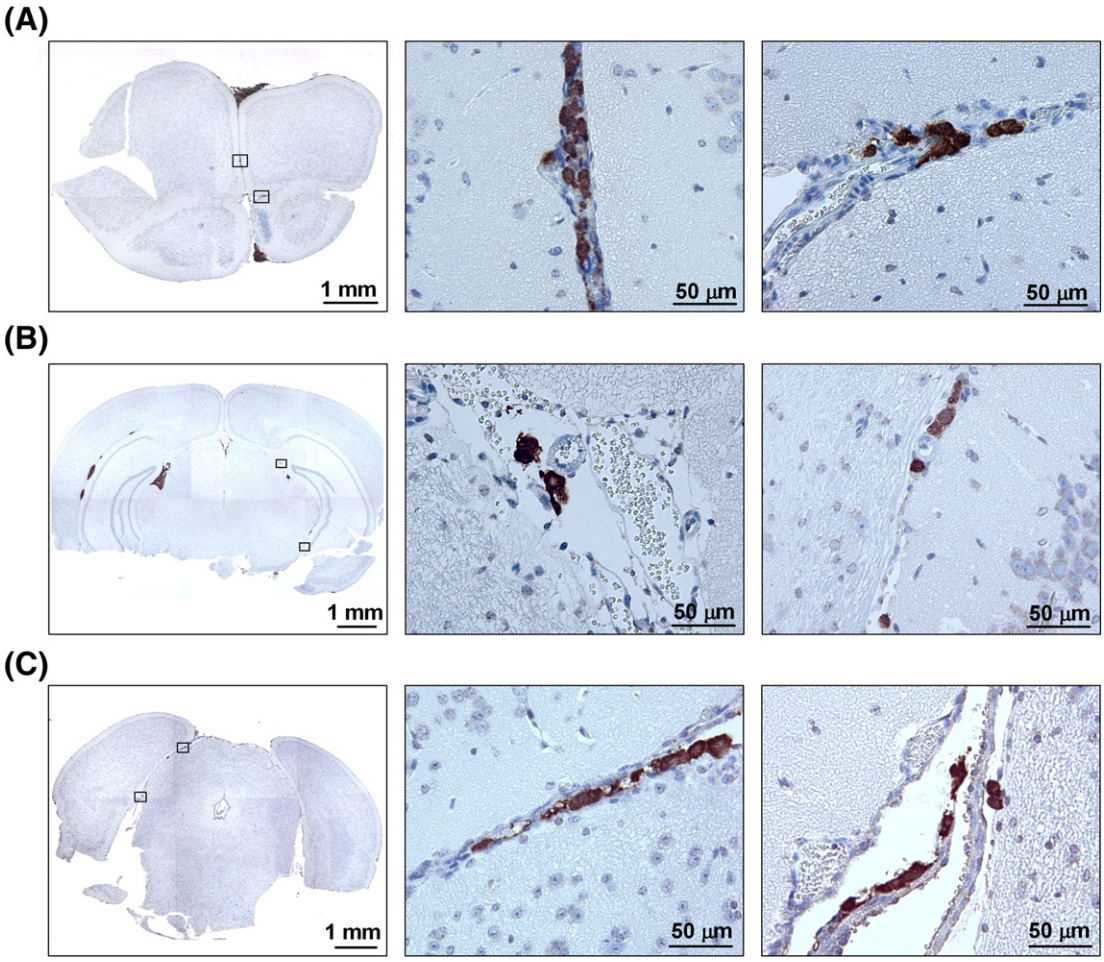

Figure 6. GFP-stained histological brain sections showing GFP-expressing melanoma cells migrating along the surfaces separating different brain compartments. (A) R-18 cells migrating between the right and left cerebral hemisphere. (B) R-18 cells migrating between the midbrain and the hippocampal region of the right cerebral hemisphere. (C) R-18 cells migrating between the left cerebral hemisphere and the midbrain. High-magnification images show areas indicated by squares in the low-magnification images.

on the cranial and caudal brain surfaces. Figure 6, *B* and *C* shows similar examples of melanoma cells located between the midbrain and the right cerebral hemisphere (Figure 6, *B*) and between the midbrain and the left cerebral hemisphere (Figure 6, *C*). These images suggest that the melanoma cells migrated actively along the surfaces separating different brain compartments. To the best of our knowledge, it has not been previously reported that melanoma cells can migrate between all these different brain compartments.

Differences in Aggressiveness and Intracranial Spread between Melanoma Lines

The melanoma lines differed significantly in aggressiveness after intracerebral cell inoculation. The mean time from inoculation to euthanization of the host mouse varied from ~17 to ~26 days (Figure 7, *A*) and was significantly longer for the D-12 and R-18 lines than for the A-07 and U-25 lines ($P < .001$). Intracerebral tumors that spread by passive transport via CSF flow developed multiple intraventricular lesions, and this route of intracranial spread was used frequently by R-18 cells and rarely by A-07 and U-25 cells (Figure 7, *B*). Active migration of tumor cells along the surfaces of vessels and brain compartments resulted in multiple meningeal lesions, and A-07 and U-25 cells spread primarily by this route, whereas this route was used less frequently by D-12 and R-18 cells (Figure 7, *C*). Taken together, these observations suggest that highly aggressive intracerebral melanoma lesions have cells with elevated capability to migrate along tissue surfaces.

Differences in Aggressiveness between Intracerebral and Intradermal Melanoma Lesions

The aggressiveness of A-07, D-12, R-18, and U-25 tumors transplanted to intradermal sites in female BALB/c *nu/nu* mice has been studied extensively in our laboratory. To compare intracerebral tumors with intradermal tumors, some results from a recent study of intradermal tumors are reproduced in Figure 7, *D–F* [23]. At the intradermal site, the four lines differed significantly in tumor growth rate ($P < .05$), and A-07 tumors showed the highest growth rate (i.e., the shortest volume doubling time), whereas U-25 tumors showed the lowest growth rate (i.e., the longest volume doubling time; Figure 7, *D*). Also, the angiogenic activity differed significantly among the four lines ($P < .05$, Figure 7, *E*), and there was a strong correlation between tumor growth rate and tumor-induced angiogenic activity ($P < .001$). Furthermore, tumor cell invasiveness measured *in vitro* in Matrigel invasion chambers differed among the lines and was significantly higher for A-07 and D-12 cells than for R-18 and U-25 cells ($P < .01$, Figure 7, *F*).

Thus, A-07 cells were highly aggressive at the intracerebral as well as the intradermal site, whereas U-25 cells were highly aggressive at

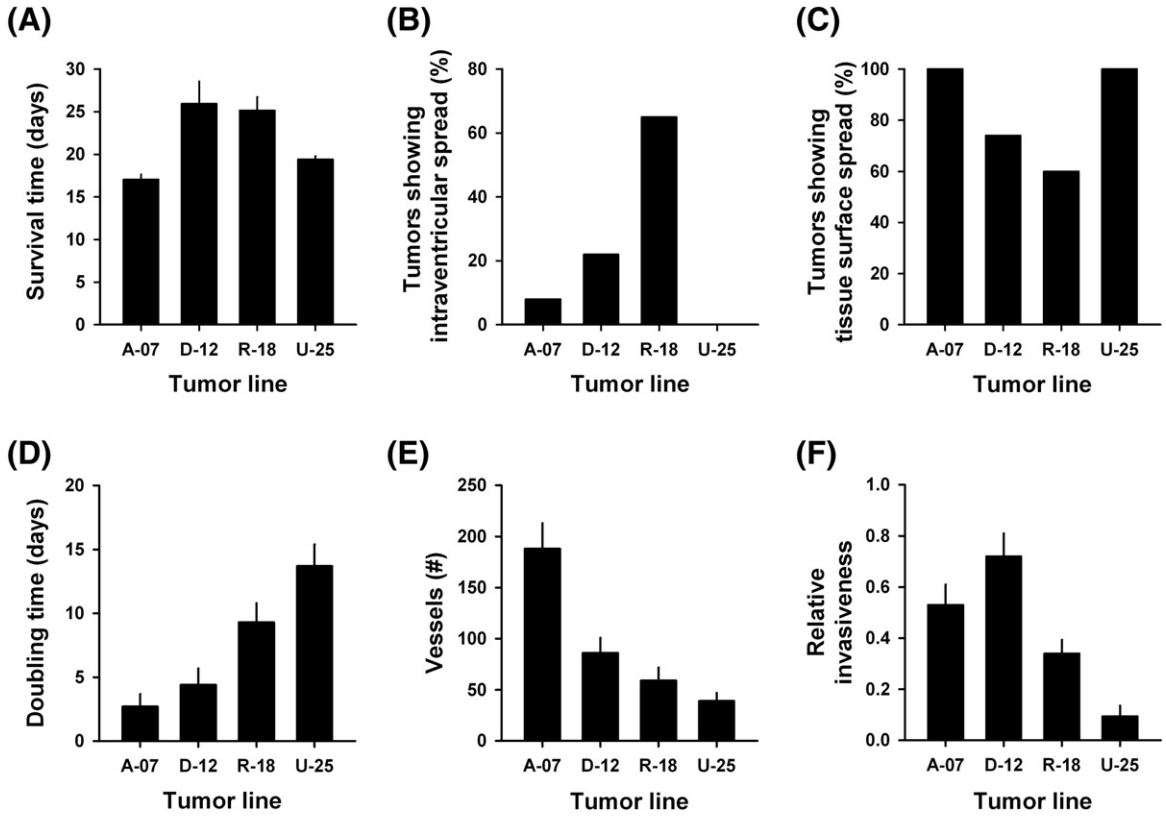

Figure 7. Aggressiveness of experimental intracerebral and intradermal melanoma lesions. (A) Mouse survival time following intracerebral inoculation of melanoma cells. Columns and bars represent mean ± SE of 20 mice. (B) Fraction of intracerebral melanomas showing metastatic spread by passive transport of tumor cells via cerebrospinal fluid flow ($n = 20$). (C) Fraction of intracerebral melanomas showing metastatic spread by active migration of tumor cells along tissue surfaces ($n = 20$). (D) Volume doubling time of intradermal melanomas. Columns and bars represent mean ± SE of 20 tumors. (E) Angiogenic potential determined by inoculating 1.0×10^6 melanoma cells intradermally and counting the tumor-oriented blood vessels 7 days later. Columns and bars represent mean ± SE of 20 tumors. (F) Relative invasiveness of melanoma cells measured *in vitro* in Matrigel invasion chambers by using Z-98 melanoma cells as a reference. Columns and bars represent mean ± SE of six experiments. The data in panels (D), (E), and (F) were reproduced from a previous publication, and experimental details are described in that publication [23].

the intracerebral site and poorly aggressive at the intradermal site. Furthermore, the aggressiveness at the intradermal site was associated with the angiogenic potential of the tumor cells, whereas the aggressiveness at the intracerebral site was associated with the capability of the tumor cells to migrate along tissue surfaces. Interestingly, there was no correlation between tumor cell migration in the brain and tumor cell invasiveness *in vitro*, suggesting that these properties of melanoma cells are governed by different mechanisms. Taken together, our observations imply that there is no correlation between the aggressiveness of melanoma lesions in the brain and in the dermis. This finding may have significant implications for the treatment of melanoma patients with advanced disease. These patients may have multiple cutaneous and brain metastases, and treatments that may be efficient against cutaneous metastases may not necessarily be efficient against brain metastases and *vice versa*. Consequently, efficient treatment of advanced melanoma may require therapeutic strategies combining different treatment modalities or different anticancer agents. Studies of A-07, D-12, R-18, and U-25 tumors suggest that treatment strategies targeting angiogenesis may be potentially useful against cutaneous metastases, whereas treatment of metastases in the brain may require treatment strategies targeting active tumor cell migration.

Conclusions

Melanoma cells are highly motile within the brain, and they can migrate to different brain regions by passive transport via CSF flow in the ventricles, by active migration along leptomeningeal and parenchymal blood vessels, and by active migration along the surfaces of the brain compartments. The different transport modes were observed in all four melanoma lines studied here, suggesting that these transport modes are common in melanoma. Consequently, intracranial migration of tumor cells may contribute significantly to the high incidence of multiple brain metastases in melanoma patients. Once melanoma cells have reached the brain, new lesions within multiple brain regions may continue to develop even in a situation where the systemic disease is controlled.

Efficient treatment strategies for melanoma patients with advanced disease may need to target cutaneous lesions as well as lesions residing within multiple regions of the brain and, hence, lesions having substantially different microenvironments [17,18]. Because the response of melanoma lesions to treatment is greatly affected by the tumor microenvironment [24,25], the development of efficient treatment strategies for melanoma patients with multiple cutaneous and brain metastases may be an immense challenge.

References

[1] McWilliams RR, Rao RD, Buckner JC, Link MJ, Markovic S, and Brown PD (2008). Melanoma-induced brain metastases. *Expert Rev Anticancer Ther* **8**, 743–755.

[2] Patel JK, Didolkar MS, Pickren JW, and Moore RH (1978). Metastatic pattern of malignant melanoma. A study of 216 autopsy cases. *Am J Surg* **135**, 807–810.

[3] Budman DR, Camacho E, and Wittes RE (1978). The current causes of death in patients with malignant melanoma. *Eur J Cancer* **14**, 327–330.

[4] Fonkem E, Uhlmann EJ, Floyd SR, Mahadevan A, Kasper E, Eton O, and Wong ET (2012). Melanoma brain metastasis: overview of current management and emerging targeted therapies. *Expert Rev Neurother* **12**, 1207–1215.

[5] Sampson JH, Carter Jr JH, Friedman AH, and Seigler HF (1998). Demographics, prognosis, and therapy in 702 patients with brain metastases from malignant melanoma. *J Neurosurg* **88**, 11–20.

[6] Raizer JJ, Hwu WJ, Panageas KS, Wilton A, Baldwin DE, Bailey E, von Althann C, Lamb LA, Alvarado G, and Bilsky MH, et al (2008). Brain and leptomeningeal metastases from cutaneous melanoma: survival outcomes based on clinical features. *Neuro Oncol* **10**, 199–207.

[7] Davies MA, Liu P, McIntyre S, Kim KB, Papadopoulos N, Hwu WJ, Hwu P, and Bedikian A (2011). Prognostic factors for survival in melanoma patients with brain metastases. *Cancer* **117**, 1687–1696.

[8] Kienast Y, von Baumgarten L, Fuhrmann M, Klinkert WE, Goldbrunner R, Herms J, and Winkler F (2010). Real-time imaging reveals the single steps of brain metastasis formation. *Nat Med* **16**, 116–122.

[9] Carbonell WS, Ansorge O, Sibson N, and Muschel R (2009). The vascular basement membrane as "soil" in brain metastasis. *PLoS One* **4**, e5857.

[10] Kusters B, Leenders WP, Wesseling P, Smits D, Verrijp K, Ruiter DJ, Peters JP, van der Kogel AJ, and de Waal RM (2002). Vascular endothelial growth factor-A(165) induces progression of melanoma brain metastases without induction of sprouting angiogenesis. *Cancer Res* **62**, 341–345.

[11] Berghoff AS, Rajky O, Winkler F, Bartsch R, Furtner J, Hainfellner JA, Goodman SL, Weller M, Schittenhelm J, and Preusser M (2013). Invasion patterns in brain metastases of solid cancers. *Neuro Oncol* **15**, 1664–1672.

[12] Hung T, Morin J, Munday WR, Mackenzie IR, Lugassy C, and Barnhill RL (2013). Angiotropism in primary cutaneous melanoma with brain metastasis: a study of 20 cases. *Am J Dermatopathol* **35**, 650–654.

[13] Rofstad EK (1994). Orthotopic human melanoma xenograft model systems for studies of tumour angiogenesis, pathophysiology, treatment sensitivity and metastatic pattern. *Br J Cancer* **70**, 804–812.

[14] Tsien RY (1998). The green fluorescent protein. *Annu Rev Biochem* **67**, 509–544.

[15] Fidler IJ (1986). Rationale and methods for the use of nude mice to study the biology and therapy of human cancer metastasis. *Cancer Metastasis Rev* **5**, 29–49.

[16] Rofstad EK and Måseide K (1999). Radiobiological and immunohistochemical assessment of hypoxia in human melanoma xenografts: acute and chronic hypoxia in individual tumours. *Int J Radiat Biol* **75**, 1377–1393.

[17] Schackert G, Price JE, Zhang RD, Bucana CD, Itoh K, and Fidler IJ (1990). Regional growth of different human melanomas as metastases in the brain of nude mice. *Am J Pathol* **136**, 95–102.

[18] Kusters B, Westphal JR, Smits D, Ruiter DJ, Wesseling P, Keilholz U, and de Waal RM (2001). The pattern of metastasis of human melanoma to the central nervous system is not influenced by integrin alpha(v)beta(3) expression. *Int J Cancer* **92**, 176–180.

[19] Amer MH, Al-Sarraf M, Baker LH, and Vaitkevicius VK (1978). Malignant melanoma and central nervous system metastases: incidence, diagnosis, treatment and survival. *Cancer* **42**, 660–668.

[20] Morris SL, Low SH, A'Hern RP, Eisen TG, Gore ME, Nutting CM, and Harrington KJ (2004). A prognostic index that predicts outcome following palliative whole brain radiotherapy for patients with metastatic malignant melanoma. *Br J Cancer* **91**, 829–833.

[21] Taillibert S, Laigle-Donadey F, Chodkiewicz C, Sanson M, Hoang-Xuan K, and Delattre JY (2005). Leptomeningeal metastases from solid malignancy: a review. *J Neurooncol* **75**, 85–99.

[22] Boyle R, Thomas M, and Adams JH (1980). Diffuse involvement of the leptomeninges by tumour–a clinical and pathological study of 63 cases. *Postgrad Med J* **56**, 149–158.

[23] Rofstad EK and Mathiesen B (2010). Metastasis in melanoma xenografts is associated with tumor microvascular density rather than extent of hypoxia. *Neoplasia* **12**, 889–898.

[24] Klemm F and Joyce JA (2015). Microenvironmental regulation of therapeutic response in cancer. *Trends Cell Biol* **25**, 198–213.

[25] Fidler IJ (2011). The role of the organ microenvironment in brain metastasis. *Semin Cancer Biol* **21**, 107–112.